



The plant immunity inducer pipecolic acid accumulates in the xylem sap and leaves of soybean seedlings following *Fusarium virguliforme* infection



Nilwala S. Abeysekara^{a,b,1}, Sivakumar Swaminathan^{a,1}, Nalini Desai^c, Lining Guo^c, Madan K. Bhattacharyya^{a,*}

^a Department of Agronomy, Iowa State University, Ames, IA, USA

^b Department of Plant Pathology and Microbiology, Iowa State University, Ames, IA, USA

^c Metabolon Inc., Durham, NC, USA

ARTICLE INFO

Article history:

Received 29 October 2015

Received in revised form

25 November 2015

Accepted 26 November 2015

Available online 28 November 2015

Keywords:

Fusarium virguliforme

Xylem sap

Metabolites

Soybean

Sudden death syndrome

Pipecolic acid

ABSTRACT

The causal agent of the soybean sudden death syndrome (SDS), *Fusarium virguliforme*, remains in infected roots and secretes toxins to cause foliar SDS. In this study we investigated the xylem sap, roots, and leaves of *F. virguliforme*-infected and -uninfected soybean seedlings for any changes in a set of over 3,000 metabolites following pathogen infection by conducting GC/MS and LC/MS/MS, and detected 273 biochemicals. Levels of many intermediates of the TCA cycle were reduced suggesting suppression of this metabolic pathway by the pathogen. There was an increased accumulation of peroxidated lipids in leaves of *F. virguliforme*-infected plants suggesting possible involvement of free radicals and lipoxygenases in foliar SDS development. Levels of both isoflavone conjugates and isoflavonoid phytoalexins were decreased in infected roots suggesting degradation of these metabolites by the pathogen to promote root necrosis. The levels of the plant immunity inducer pipecolic acid (Pip) and the plant hormone salicylic acid (SA) were significantly increased in xylem sap (in case of Pip) and leaves (in case of both Pip and SA) of *F. virguliforme*-infected soybean plants compared to the control plants. This suggests a major signaling role of Pip in inducing host defense responses in above ground parts of the *F. virguliforme*-infected soybean. Increased accumulation of pipecolic acid in foliar tissues was associated with the induction of *GmALD1*, the soybean homolog of Arabidopsis *ALD1*. This metabolomics study generated several novel hypotheses for studying the mechanisms of SDS development in soybean.

© 2015 Elsevier Ireland Ltd. All rights reserved.

1. Introduction

Interactions of pathogens with plants lead to an array of changes in transcriptomes, proteomes, and metabolomes in both hosts and pathogens. Metabolic changes are well known for their roles in defending plants from invading pathogens. For example, phytoalexins and lignins are two long studied secondary

metabolite classes that are considered to play major roles in plant defense. Depending on the host cultivar, there can be large qualitative differences in the accumulation of plant metabolites in response to different pathogen infections [1]. For instance, *Fusarium oxysporum*-infected *Brassica rapa* plants have been shown to accumulate more phenylpropanoids, flavonoids, and fumaric acid than those infected with other pathogenic fungi like *Aspergillus niger* and *Leptosphaeria maculans* [1]. Degradation of isoflavonoid phytoalexins by pathogens has been shown to be necessary for disease development [2].

Investigation of the global changes of metabolites can help answer plant biological questions. The utility of metabolomics in dissecting plant-fungal interactions has been reviewed recently [3]. Metabolic profiling was used to study the basal metabolism in *Fusarium* spp. [4]. The roles of small metabolites, such as methyl salicylate, azelaic acid, and pipecolic acid, in the expression of systemic acquired resistance have recently been considered [5]. Xylem

Abbreviations: BLOB, binary large object; BSTFA, bistrimethyl-silyl-trifluoroacetamide; ESI, electrospray ionization; FT-ICR, Fourier transform ion cyclotron resonance; 13-HODE, 13-(S)-hydroxyoctadecadienoic acid; 9-HODE, 9-Hydroxy-10,12-octadecadienoic acid; LAN, local area network; LIMS, laboratory information management system; LIT, linear ion-trap; Pip, pipecolic acid; QC, quality control; SDS, sudden death syndrome.

* Corresponding author: Fax: +1 515 294 1363.

E-mail address: mbhattac@iastate.edu (M.K. Bhattacharyya).

¹ These authors contributed equally.

sap is known to be involved in long-distance signaling in response to pathogen infection [6]. Changes are observed in xylem sap proteomes and metabolomes in response to abiotic and biotic stresses [6–8]. Pathogen infections can result in increases in phenolic compounds [9] and/or salicylic acid and its derivatives in the xylem sap [10]. Changes in the contents of phenolic and indolic compounds, amino acids, nitrogen compounds, disaccharides, glucosinolates and molecules that lead to an increase in reactive oxygen species have been observed in *Arabidopsis thaliana* infected with *Pseudomonas syringae* pv. tomato [11].

Sudden death syndrome (SDS) is a soybean fungal disease that can cause drastic annual yield losses of nearly 300 million dollars [12]. In North America, this disease is caused solely by *Fusarium virguliforme*, formally known as *F. solani* (Mart.) Sacc. f. sp. *glycines*; whereas, in South America five different *Fusarium* species including *F. virguliforme* are known to cause the disease [13–15]. *F. virguliforme* is a hemi-biotrophic, soil borne, asexually propagated fungus possessing only one mating gene idiomorph, *MAT1-1*; in contrast, *F. tucumaniae*, one of the SDS pathogens in South America, comprises two idiomorphs each having either the *Mat1-1* or *Mat1-2* gene and is therefore able to sexually propagate [13,16]. *F. virguliforme* causes root necrosis and has never been detected in diseased foliar tissues. Host-selective toxins produced by the fungus have been hypothesized to cause foliar SDS symptoms as the pathogen restricted to infected soybean roots [17–19]. Recently, a major *F. virguliforme* toxin FvTox1 has been shown to induce foliar SDS in soybean [20–22]. In addition, five minor candidate toxins have been detected in xylem sap proteomes [7]. Thus, it is becoming apparent that multiple host-selective toxins produced by *F. virguliforme* could be transported to the leaves via the vascular system to cause foliar SDS in soybean [7,20–22].

SDS is an emerging disease with no known genes conferring complete resistance against the SDS pathogen, *F. virguliforme*. Toxin-induced foliar SDS is the highly destructive component of the disease and can lead to total yield losses. To date, there are no fungicides available for controlling this disease. Therefore it is essential to understand the mechanisms of disease development in order to design appropriate SDS management practices. In this study we monitored the accumulation patterns of 273 biochemicals in roots, xylem sap and leaves of *F. virguliforme*-infected and uninfected SDS-susceptible soybean cultivar “Spencer” to determine if there are any biochemicals that are accumulated during SDS development. Elevated levels of the plant immunity inducer pipelicolic acid were observed in the xylem sap and leaves of *F. virguliforme*-infected soybean plants. In addition, the levels of peroxidated lipids were increased in leaves of *F. virguliforme*-infected plants, compared to those of uninfected soybean plants. This suggests a possible involvement of free radicals and lipoxygenases in developing foliar SDS symptoms following root infection of soybean with *F. virguliforme*.

2. Materials and methods

2.1. Inoculum preparation, plant material, and xylem sap collection

The cultivar “Spencer”, a highly *F. virguliforme*-susceptible soybean cultivar, was used in this study. Mixed inoculum from two *F. virguliforme* isolates, Scott and Clinton, was prepared in sorghum meal as described by Hartman et al. [23]. Mixed inoculum was used to increase the disease pressure. The isolates were grown in 1/3 strength potato dextrose agar (PDA) prior to inoculation of sorghum meal. Detailed descriptions of growth conditions of the plants, inoculum preparation, and xylem sap collection are reported by Abeyssekara and Bhattacharyya [7]. In brief, 120 seedlings were

grown in soil mixed with either the *F. virguliforme* inocula grown in sorghum as the treatment or with just the sorghum meal as the control [23,24]. Approximately between 14 and 21 days after emergence, xylem sap was collected from the plants showing uniform levels of foliar disease severity. The experiment was repeated four more times. Roots and leaves from each of the infected and uninfected seedlings were collected separately, ground in liquid nitrogen, and stored at -80°C along with the xylem sap samples until analysis. The experiment was repeated three more times for collecting leaf and root samples to conduct RT-PCR analysis for a few selected genes.

2.2. Sample preparation

Metabolomic analysis of the xylem sap samples was carried out at Metabolon Inc., Durham, NC, USA. The sample preparation process was carried out using the automated MicroLab STAR[®] system from Hamilton Company. Recovery standards were added prior to extraction for quality control (QC) purposes. Sample preparation was conducted using a proprietary series of organic and aqueous extractions to remove the protein fraction while allowing maximum recovery of small molecules. The resulting extract was divided into two fractions; one for analysis by LC and the other one for analysis by GC. Samples were placed briefly on a TurboVap[®] (Zymark) to remove the organic solvent. Each sample was then frozen and dried under vacuum prior to reconstitution in another solvent depending on the following analysis (see Sections 2.3 and 2.4).

2.3. Liquid chromatography/mass spectrometry (LC/MS, LC/MS/MS) and accurate mass measurement

The LC/MS was conducted on a Waters ACQUITY UPLC and a Thermo-Finnigan LTQ mass spectrometer, which consisted of an electrospray ionization (ESI) source and a linear ion-trap (LIT) mass analyzer. The sample extract was split into two aliquots, dried, then reconstituted in acidic or basic LC-compatible solvents, each of which contained at least 11 injection standards at fixed concentrations. One aliquot was analyzed using acidic conditions optimized for positive ion detection and the other one using basic conditions optimized for negative ion detection. After injection, each sample aliquot was separated on separate acid/base dedicated 2.1 mm \times 100 mm Waters BEH C18 1.7 μm particle columns (Waters, Milford, MA, USA). Extracts reconstituted in acidic conditions were eluted using a gradient of water and methanol containing 0.1% formic acid, while for elution of the basic extracts, the gradient of water and methanol contained 6.5 mM ammonium bicarbonate. For ions with counts greater than 2 million, an accurate mass measurement was performed. Accurate mass measurements could be made on the parent ion as well as on the fragments. The typical mass error was less than 5 ppm. Ions with less than two million counts require a greater amount of effort to characterize. Fragmentation spectra (MS/MS) were typically generated in data dependent manner, but when necessary, targeted MS/MS was also employed, such as in the case of metabolites with lower level signals.

2.4. Gas chromatography/mass spectrometry (GC/MS)

The samples destined for GC/MS analysis were dried by vacuum desiccation for a minimum of 24 h prior to derivatization under nitrogen using bistrimethyl-silyl-trifluoroacetamide (BSTFA). A 20 m \times 0.18 mm (0.18 mm film phase consisting of 5% phenyldimethyl silicone) GC column (Thermo Finnegan, San Jose, CA, USA) was used and the temperature ramp used was from 40° to 300°C in a 16 min period. Samples were analyzed on a

Thermo-Finnigan Trace DSQ fast-scanning single-quadrupole mass spectrometer using electron impact ionization.

2.5. Bioinformatics

The informatics system consisted of four major components: (i) the laboratory information management system (LIMS); (ii) the data extraction and peak-identification software, a modified version of “Array Studio” software (OmicSoft Corporation, Cary, NC, USA); (iii) data processing tools for QC and compound identification [25,26]; and (iv) a collection of information interpretation and visualization tools for use by data analysts [25,26]. The hardware and software foundations for these informatics components were the local area network (LAN) backbone, and a database server running Oracle 10.2.0.1 Enterprise Edition.

2.6. Data extraction and quality assurance

Information from the data extraction of the raw mass spectrometry data files was loaded into a relational database and manipulated without resorting to binary large object (BLOB) manipulation. Once in the database, the information was examined and appropriate QC limits were imposed. Peaks were identified using Metabolon’s proprietary peak integration software, and component parts were stored in a separate and specifically designed complex data structure [25,26].

2.7. Compound identification

Compounds were identified by comparison to >3,000 library entries of purified standards. Identification of chemical entities was based on comparison to metabolomic library entries of purified standards. The combination of chromatographic properties and mass spectra gave an indication of a match to the specific compound or an isobaric entity [25,26].

2.8. Data imputation and statistical analysis

The missing value for a given metabolite was imputed with the observed minimum detected value, based on the assumption that they were below the limits of detection sensitivity of the instrument. Statistical analysis of the data was performed using JMP (SAS, <http://www.jmp.com>) and “R” (<http://cran.r-project.org/>). Following log transformation and imputation with minimum observed values for each compound, Welch’s two sample *t*-tests was used to identify biochemicals that differed significantly between experimental groups [27]. An estimate of the false discovery rate (*q*-value) [28] was also calculated to account for the multiple comparisons that normally occur in metabolomic-based studies.

2.9. Visualization of the study data

For the convenience of data visualization, the raw area counts for each biochemical compound were re-scaled by dividing the value for a specific biochemical in each sample by the median value observed for that specific biochemical (median scaled). Box plots were used to convey the spread of the data with 50% of the data points closest to the median represented by shaded boxes and whiskers reporting the overall range of the data. The solid horizontal bar within a shaded box represents the median while the + indicates the mean values. Data were scaled such that the median value measured across all samples was set to 1.0. Any outliers were shown as dots outside the whiskers of the plot [25,26].

2.10. RT-PCR analysis

Total RNA was extracted from the 14-day old leaves and roots of uninfected and infected soybean plants using the SV Total RNA Isolation System (Promega, Madison, WI, USA). RNAs were eluted from the column in nuclease-free water, and aliquots were stored at -80°C prior to analysis. From RNA, first strand cDNA amplification was carried out with Superscript III reverse transcriptase enzyme kit (Invitrogen, Life Technologies, Grand Island, NY, USA) by using an oligo(dT)₂₀ primer. The PCR was carried out with the Taq DNA polymerase (Invitrogen, Life Technologies, Grand Island, NY, USA) by using the cDNAs as template. The PCR amplification conditions were as follows: 30 PCR cycles of denaturation temperature at 94°C for 30 s, re-annealing at 52°C for 30 s, and extension at 72°C for 40 s followed by a final extension cycle of 10 min at 72°C . The PCR products were ran on 1% agarose gel and photographed with a gel doc imaging system (FOTODYNE Incorporated, Hartland, WI, USA).

2.11. Molecular phylogenetic analysis of ALD1 proteins

The evolutionary relationship of ALD1 proteins of Arabidopsis with other species was inferred by using the Maximum Likelihood method with bootstrap (1050 replicates) by analyzing the MUSCLE alignment of the reported ALD1 sequences. Evolutionary analyses were conducted in MEGA7 software program (Center for Evolutionary Medicine and Informatics, Tempe, AZ, USA). The tree with the highest log likelihood (-5296.8872) is shown. Initial tree(s) for the heuristic search were obtained automatically by applying Neighbor-Join and BioNJ algorithms to a matrix of pairwise distances estimated using a JTT model, and then selecting the topology with superior log likelihood value. The analysis involved 5 amino acid sequences. All positions with less than 95% site coverage were eliminated with fewer than 5% alignment gaps, missing data, and ambiguous bases at any position. There were 449 positions in the final dataset.

3. Results and discussion

In this study we investigated the metabolomes of root, xylem sap, and leaves of *F. virguliforme*-infected and uninfected plants of an SDS susceptible soybean cultivar, “Spencer.” A total of 273 biochemicals were detected in this study. The number of biochemicals with statistical significance at $p \leq 0.05$ and $0.05 < p < 0.1$ are summarized in Table 1. An overview of the major biochemicals is presented as a heat map in Fig. 1. A more detailed heat map can be found in Fig. S1. The data of all three matrices (viz., leaves, xylem sap and roots) were treated as stemming from a single experiment (Fig. S1). Differential accumulation of many metabolites between *F. virguliforme*-infected and -uninfected soybean plants was observed for all three matrices.

Supplementary material related to this article found, in the online version, at <http://dx.doi.org/10.1016/j.plantsci.2015.11.008>.

3.1. Altered accumulation of isoflavonoids and their conjugates following *F. virguliforme* infection

In this study, we observed a general decline in isoflavone biosynthetic precursors, isoliquiritigenin and liquiritigenin, and the isoflavone conjugate daidzin (daidzein 7-O-glucoside) in *F. virguliforme*-infected root tissues as compared to control root tissues (Fig. 2). The pathogen has been shown to induce the accumulation of the isoflavonoid glyceollin in infected hairy soybean roots developed from an SDS resistant cultivar [29]. The isoflavone, formononetin but not coumestrol, was substantially elevated in both xylem sap and leaf samples of infected plants as compared to that of the control plants. Daidzein, the precursor of formononetin, was

Table 1
Summary of the number of compounds which significantly differ between experimental groups either at $p \leq 0.05$ or $0.05 < p < 0.10$ (Welch's two-sample *t*-test) within a pool of 273 plant metabolites termed 'biochemicals' in this study.

Welch's two sample <i>t</i> -tests	I-LEAF-C-LEAF	I-SAP-C-SAP	I-ROOT-C-ROOT
Total number of biochemicals with $p \leq 0.05$	29	21	1
Biochemicals ($\uparrow \downarrow$)	23 6	3 18	1 0
Total number of biochemicals with $0.05 < p < 0.10$	25	19	3
Biochemicals ($\uparrow \downarrow$)	21 4	4 15	0 3

C, Control; I, Infected.

Numbers in bold font are the number of biochemicals that were up-regulated and the ones without bold font are the number of biochemicals that were down-regulated.

also significantly more abundant in infected leaf tissues than in the control leaf tissues (Fig. 2). Increased levels of both daidzein and formononetin were also recorded in xylem sap of *F. virguliforme*-infected plants compared to controls. We observed significantly lower levels of coumestrol and daidzin in infected roots as compared to the uninfected roots.

Phytoalexin biosynthesis is a general defense response, and soybean leaves recognize *F. virguliforme* toxin-induced disease symptoms as pathogen invasion or recognize toxins as effectors to activate the isopropanoid biosynthetic pathway for phytoalexins accumulation. A recent transcriptomic study demonstrated that genes involved in phytoalexin biosynthesis are expressed or induced in leaves following treatment of soybean seedlings with *F. virguliforme* culture filtrates containing toxins [30].

3.2. Increased levels of free and peroxidated fatty acids accumulate in soybean leaves following *F. virguliforme* infection

An increase in free fatty acids [2-hydroxypalmitate, azeolate (nonanedioate), caproate (6:0), oleate (18:1n9), linoleate

(18:2n9), palmitate (16:0), sebacate (decanedioate)] including some peroxidated fatty acids [13-(S)-hydroxyoctadecadienoic acid (13-HODE)+9-hydroxy-10,12-octadecadienoic acid (9-HODE), 9, 10-hydroxyoctadec-12(Z)-enoic acid [9-hydroxyoctadec-12(Z)-enoic acid, 10-hydroxyoctadec-12(Z)-enoic acid, or 9,10-dihydroxyoctadec-12(Z)-enoic acid], 13S-hydroperoxy-9Z,11E,15Z-octadecatrienoate, 12,13-epoxy-9-keto-10 (trans-octadecenoate)] were observed in leaf samples of infected plants as compared to that in uninfected controls (Fig. 3). The increased levels of free fatty acids suggest an increase in membrane degradation triggered by *F. virguliforme* toxins through unknown mechanisms, which could include fatty acid peroxidation via reactive oxidative species (ROS) or by lipoxygenases (LOX) [31]. Peroxidated fatty acids are oxidized metabolites of linoleic acid and are markers of membrane lipid damage caused in the presence of excess ROS or LOX activity. Additionally, LOX may also be involved in degradation of linoleic acid to the oxo-epoxyoctadecenoic acid [32]. Lipid peroxidation leads to generation oxylipins that have been shown to have signaling function across the kingdoms, both animal and plants [33]. Recently, Aliferis et al. [34] reported in their

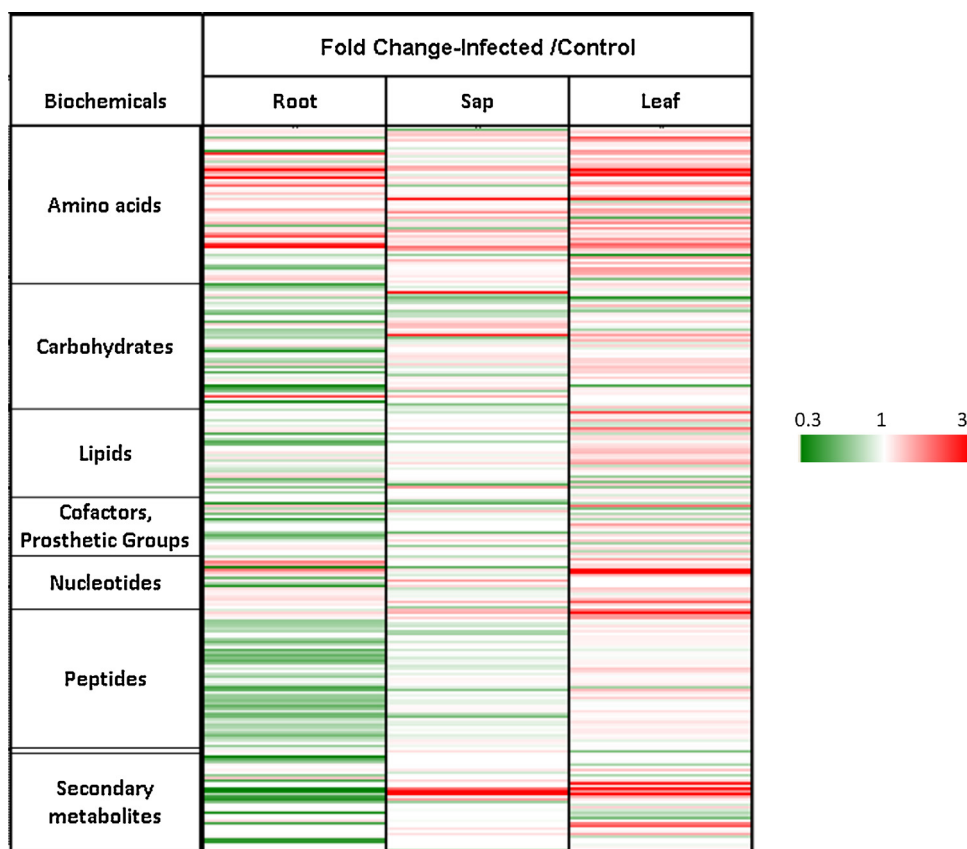


Fig. 1. The heat map showing the fold changes in major biochemicals in roots, xylem sap, and leaves of soybean seedlings infected with *F. virguliforme*. The fold changes were formatted in a graduated three-color system; green = 0.33 (three fold decrease), white = 1 (no change between the groups), and red = 3 (three-fold increase). Each line represents a metabolite.

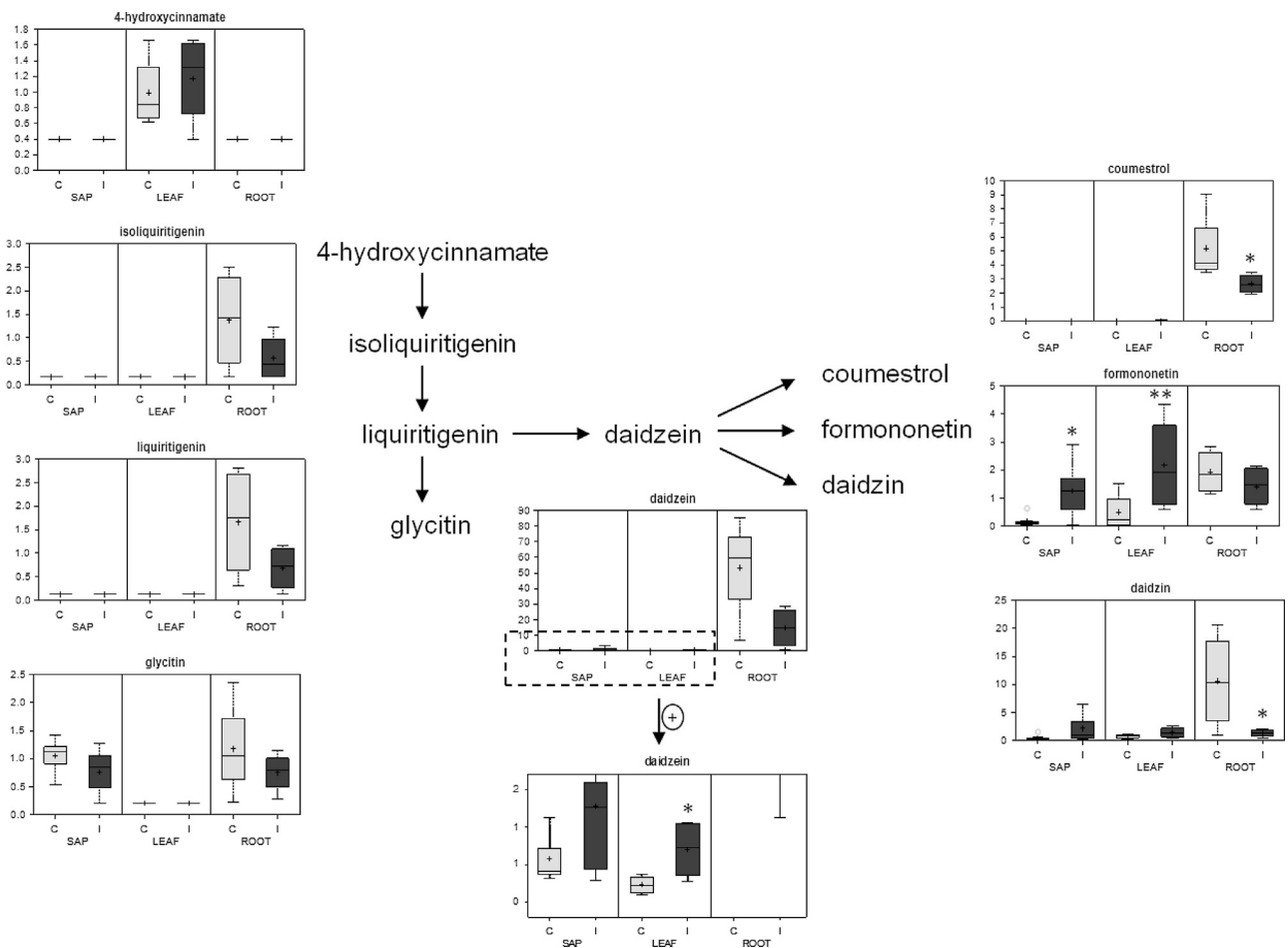


Fig. 2. Altered accumulation of conjugates and isoflavonoid metabolites in leaves and roots of *F. virguliforme*-infected as compared to the control plants. Formononetin levels were increased in both the xylem sap and leaves of the *F. virguliforme*-infected plants * $p \leq 0.1$; ** $p \leq 0.05$. C, Control; I, Infected.

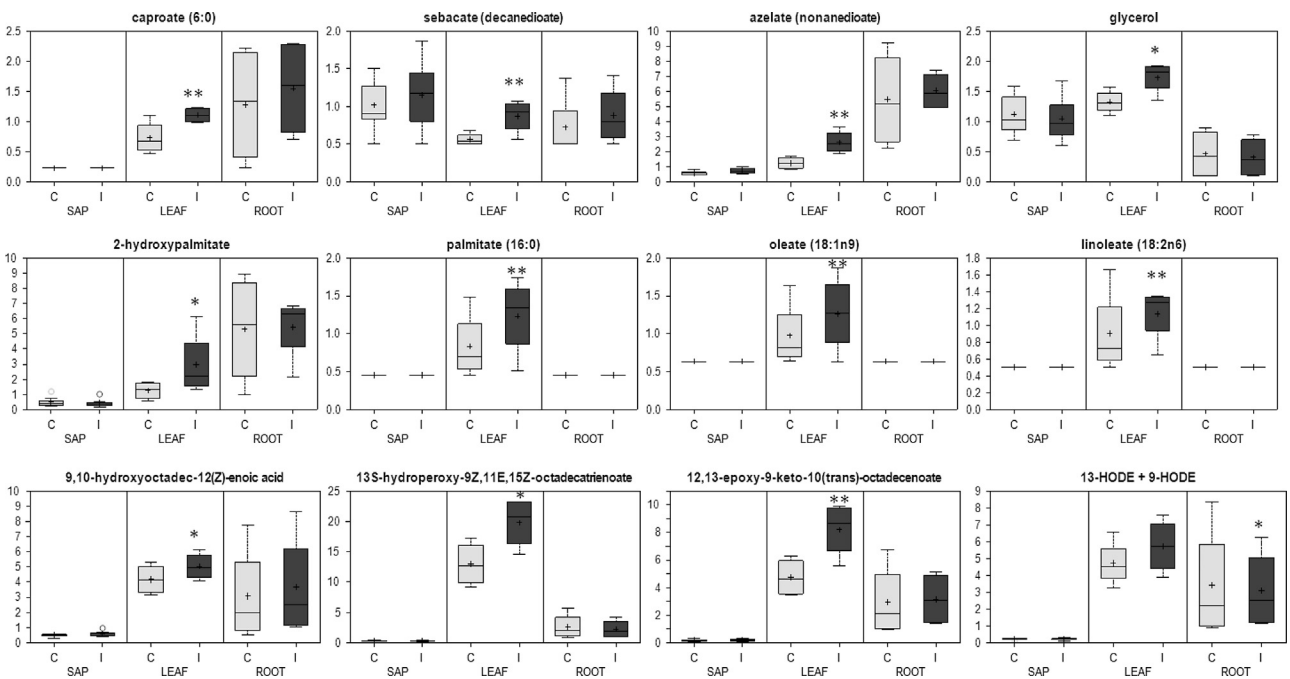


Fig. 3. Elevated free fatty acids in leaves of *F. virguliforme*-infected as compared to the *F. virguliforme*-uninfected soybean plants. HODE levels were decreased in the roots of the *F. virguliforme*-infected plants * $p \leq 0.1$; ** $p \leq 0.05$. C, Control; I, Infected.

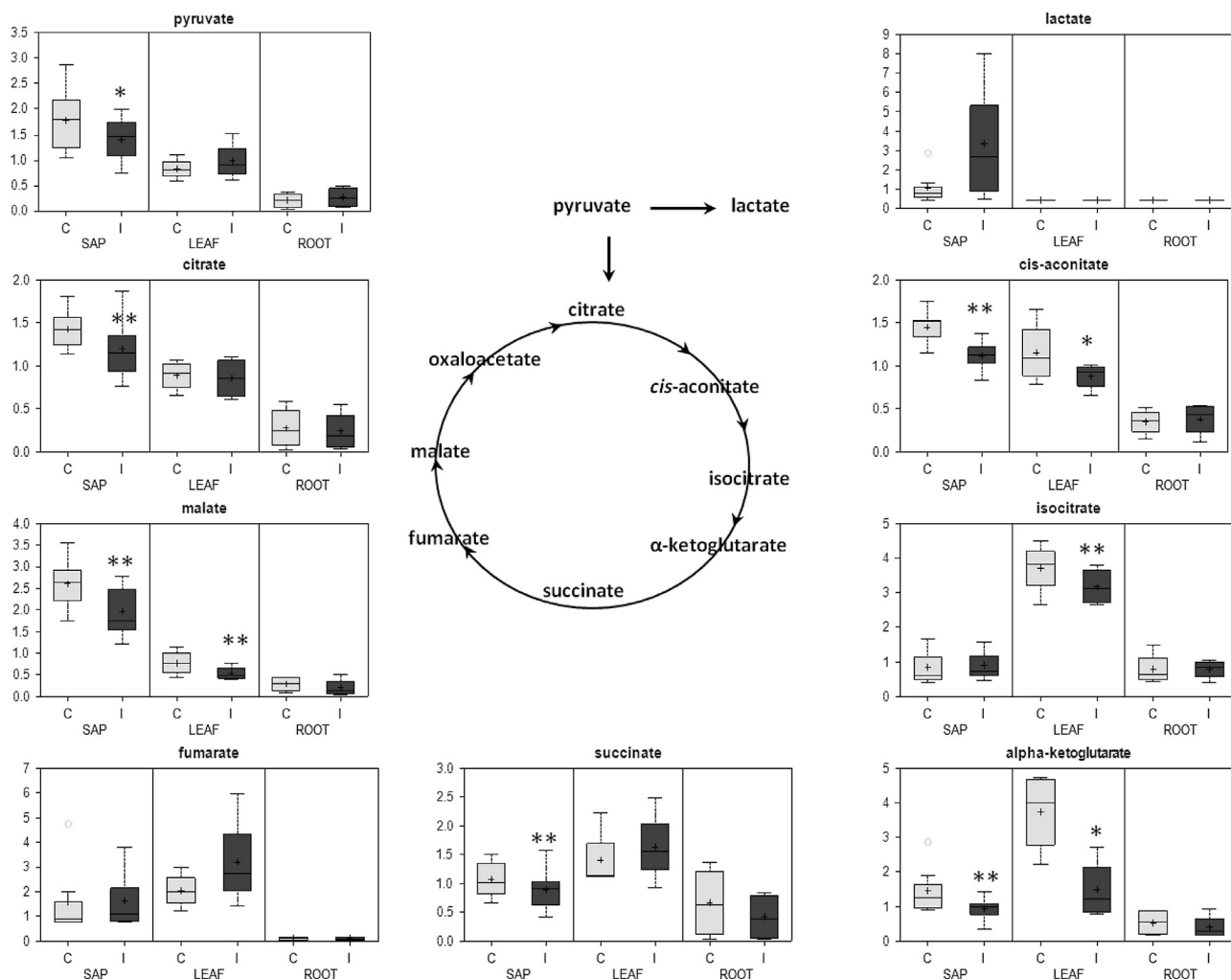


Fig. 4. General reduction in the levels of intermediate metabolites of the TCA cycle in xylem sap and leaves of soybean plants following *F. virguliforme* infection. * $p \leq 0.1$; ** $p \leq 0.05$. C, Control; I, Infected.

metabolomics study on the soybean-*Rhizoctonia solani* interaction various oxylipin species enzymatically produced and possessing a plant signaling function which were differentially regulated by pathogen infection.

The key *F. virguliforme* toxin, FvTox1, initiates foliar SDS in presence of light [20]. It has been previously shown that rapid degradation of the RubisCo large subunit and the accumulation of free radicals occur in soybean leaves exposed to *F. virguliforme* toxins and light implicating that photosynthesis could be negatively affected by the pathogen toxins [35]. The accumulated free fatty acids in leaves of *F. virguliforme*-infected compared to control plants might get converted to the corresponding oxidized products by ROS produced via the direct or indirect action of fungal toxins such as FvTox1. It is plausible that *F. virguliforme* toxins utilizes jasmonic acid to cause senescence and disease development, a mechanisms reported to be used by *F. oxysporum* to cause disease in Arabidopsis [36]. Further studies are warranted to test this hypothesis and to disentangle the possible roles of the free fatty acids in foliar SDS development.

3.3. Decreased levels of intermediates of the tricarboxylic acid cycle in xylem sap and leaves following *F. virguliforme* infection

Decreased accumulation of intermediates of the tricarboxylic acid (TCA) cycle, viz., α -ketoglutarate, cis-aconitate, citrate, malate,

and succinate as well as pyruvate in xylem sap, and α -ketoglutarate, cis-aconitate, isocitrate, and malate in leaves of the *F. virguliforme*-infected as compared to the uninfected plants were observed (Fig. 4). This overall decrease in intermediates of the TCA cycle was associated with an increase in lactate in xylem sap of *F. virguliforme*-infected as compared to the uninfected plants. Depletion of pyruvate levels most likely led to reduced accumulation of intermediates of the TCA cycle in xylem sap of *F. virguliforme*-infected plants.

3.4. Increased levels of allantoin and allantoic acid in xylem sap and leaves following *F. virguliforme* infection

The levels of allantoin and allantoic acid were significantly higher in leaf samples of infected plants than in the controls (Fig. 5). The level of allantoic acid was also elevated in the xylem sap. Ureides, allantoin, and allantoic acid are well known nitrogen carriers in plants. Legumes have a sophisticated symbiotic relationship with nitrogen fixing microorganisms. *Rhizobia* inhabit roots and provide nitrogen to the plants, and plant provides C4 carbon metabolites to the microbial TCA cycle for generating energy. The products of nitrogen fixation, mainly asparagine or allantoin and allantoic acid, are transported to the rest of the plant, for use in metabolic processes or for storage. These molecules also play a role in the co-ordinate regulation of nitrogen assimilation and energy

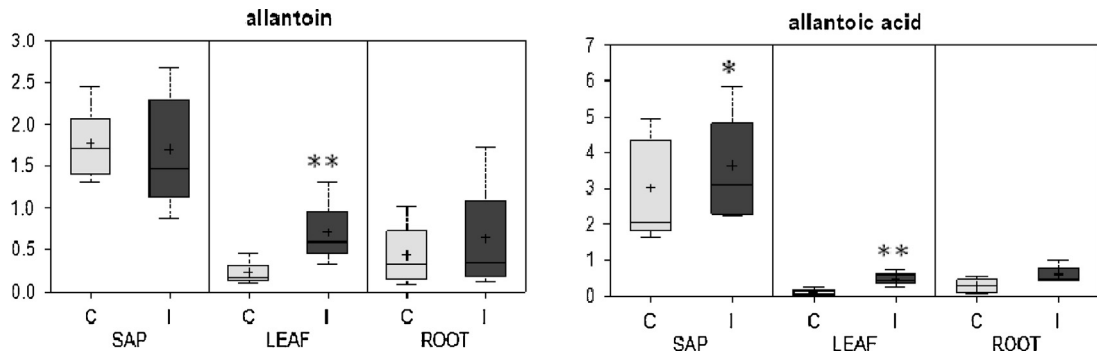


Fig. 5. Increased levels of nitrogen-rich metabolites in xylem sap and leaves of soybean plants following *F. virguliforme* infection. * $p \leq 0.1$; ** $p \leq 0.05$. C, Control; I, Infected.

expenditure in the plant. It has been suggested that the signals in plant response to pathogen infection may be similar to those produced in its response to symbiotic microbes [37]. For example, the isoflavones daidzein, formononetin and coumestrol not only accumulate after *F. virguliforme* infection, but also modulate the expression of *Nod* genes required for the establishment of nodules in legumes [38,39].

As in our investigation of the soybean-*F. virguliforme* interaction, a recent metabolomics study of the related soybean-*F. tucumaniae* interaction also revealed increases in the levels of nitrogen-containing compounds and decreases in levels of the intermediates of the TCA cycle [40]. The observation of increased nitrogen carrier accumulation in sap and leaves of *F. virguliforme* infected plants is interesting and raises several questions for further study. This host response following *F. virguliforme* infection is comparable to the one observed following colonization by plant symbiotic microorganisms to enhance nitrogen assimilation. It is very unlikely that there was any enhanced nitrogen fixation by symbiotic microorganisms because soil was steam-sterilized prior to inoculation. This observation could imply that increased nitro-

gen assimilation may be a consequence of shared mechanism(s) used by soybean in response to invasion by pathogenic and symbiotic microorganisms. It appears also plausible that plants initiate resource re-allocation processes after both pathogen and symbiont colonization for the biosynthesis of plant protectant molecules during pathogen invasion.

3.5. Elevation in the levels of the plant immunity inducers pipecolic and salicylic acid

High levels of pipecolic acid (Pip), a catabolite of lysine, which has been reported to act as an osmo-protectant, was elevated in both xylem sap and leaves of infected plants (Fig. 6). Increased accumulation of Pip was associated with a decrease of its precursor lysine in the xylem sap. Pip has recently been shown to be a critical regulator of inducible plant immunity [41]. Upon pathogen recognition, Pip accumulates in the petiole exudates of infected leaves and induces systemic acquired resistance (SAR) in *Arabidopsis* [41]. Accumulation of Pip in leaves in response to pathogen recognition has been previously reported in several plant species

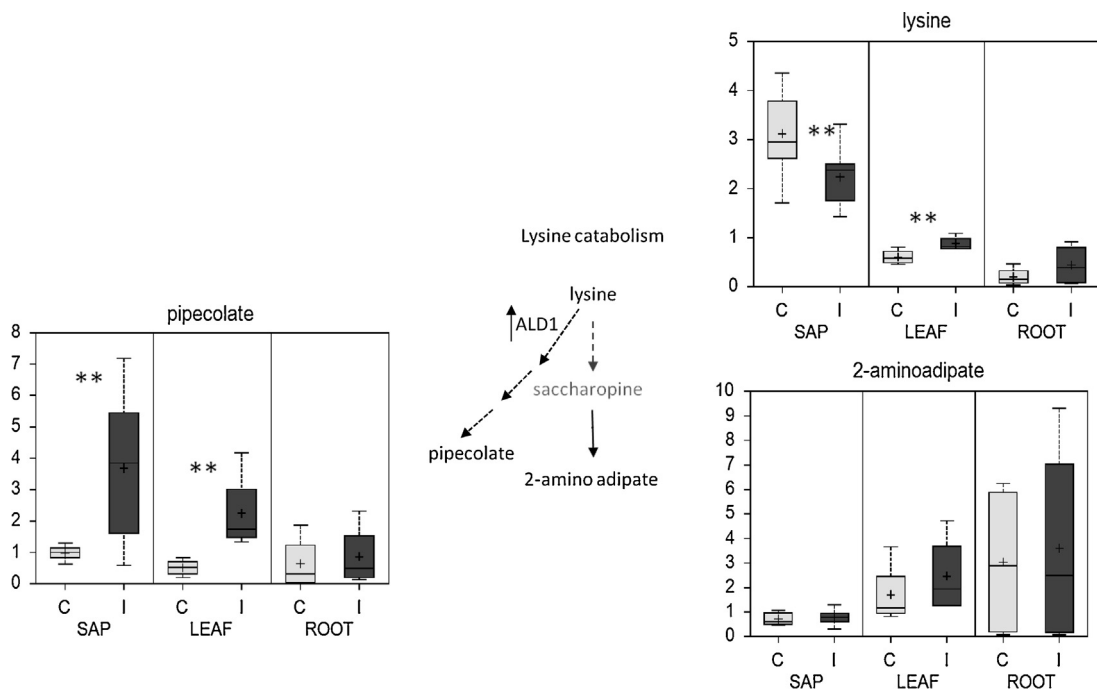


Fig. 6. Increased accumulation of pipecolate levels in xylem sap and leaves of *F. virguliforme*-infected as compared to the control soybean plants. Lysine levels were decreased in the xylem sap while increased in the leaves of *F. virguliforme*-infected plants. ** $p \leq 0.05$. C, Control; I, Infected.

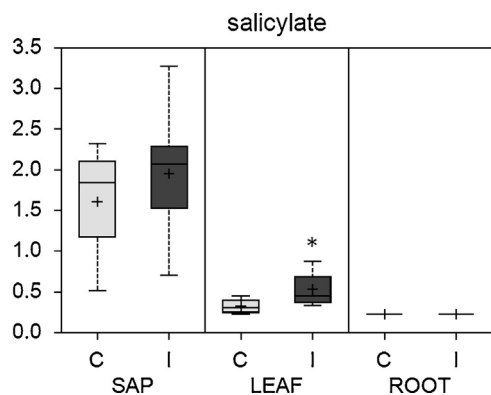


Fig. 7. Increased accumulation of salicylate levels in leaves of the *F. virguliforme*-infected as compared to the control soybean plants. * $p \leq 0.1$. C, Control; I, Infected.

including soybean [42,43,44]. It positively regulates salicylic acid (SA) biosynthesis [42].

SA levels were also elevated in *F. virguliforme*-infected leaf tissues compared to that in leaves of uninfected plants (Fig. 7). However, no significant difference was observed between salicylic acid levels of the xylem sap of infected and the uninfected soybean plants (Fig. 7). SA is a signal for the activation of disease resistance responses and also generation of long lasting and broad-spectrum systemic acquired resistance in soybean and other plant species [45]. Our data suggest that SA is induced in response to toxin-induced foliar SDS symptoms in soybean. Presumably SA accumulates due to recognition of general defense-related signals from the toxin-induced foliar SDS symptoms characterized by rapid cell death. Alternatively, it may be possible that Pip uploaded from xylem sap may signal for SA synthesis in leaves of *F. virguliforme*-infected soybean plants [41]. Further study is warranted to determine whether these important metabolites might serve as a plant signal to defend in foliar tissues as a result of the: (i) recognition of toxins as effectors by elusive soybean toxin receptors in leaves, or (ii) outcomes of the complex interaction of *F. virguliforme* with soybean roots, or (iii) both processes (i) and (ii) mentioned above.

Increased accumulation of Pip in xylem sap of infected soybean plants suggests that the molecule may be transported to apical parts of the soybean plants through xylem to serve as a signal to initiate defense responses [41]. In leaves of *F. virguliforme* infected plants, the increased Pip accumulation results from Pip transport via the xylem sap because the lysine content in leaves of diseased plants was increased while that for xylem sap went down. However, we cannot rule out the possibility of the lysine biosynthesis pathway being induced by its catabolism to Pip and its increased demand in leaves during defense responses.

To determine if Pip is synthesized in leaf tissues, we investigated the gene encoding the regulatory enzyme of Pip biosynthesis, LL-diaminopimelate aminotransferase. In soybean, we identified four genes that showed high sequence identity to Arabidopsis *ALD1*. One of these genes, *GmALD4* (Glyma.14G167600) (Supplementary Table 1) is most likely a pseudogene because it encodes a truncated protein and we did not detect any transcripts for this gene. We studied the other three genes for their steady state transcript levels (Table 2; Fig. 8; Supplementary Table 1). *GmALD1* with the highest similarity to Arabidopsis *ALD1* was induced in the leaves of *F. virguliforme*-infected soybean plants. Phylogenetic analysis of Arabidopsis *ALD1* and its homologs revealed that *GmALD1* grouped with Arabidopsis *ALD1*, and one Arabidopsis *ALD1* homolog each from *Medicago truncatula*, *Oryza sativa* and *Zea mays* in a clade (Fig. 9). Our results suggest that most likely *GmALD1* is orthologous to Arabidopsis *ALD1* and the Pip biosynthetic pathway is induced in

Table 2
ALD1 homologs^a of different plant species.

Species	Gene ID*	% Similarity to AT2G13810
<i>Arabidopsis thaliana</i>	AT2G13810 (<i>ALD1</i>)	–
<i>A. thaliana</i>	AT4G33680	67.3
<i>Glycine max</i>	Glyma.08G180600	72.8
<i>G. max</i>	Glyma.08G063500	66.9
<i>G. max</i>	Glyma.07G185700	66.7
<i>G. max</i>	Glyma.14G167600	21.9 ^b
<i>Oryza sativa</i>	LOC_Os03g18810	66.4
<i>O. sativa</i>	LOC_Os03g09910	63.6
<i>Zea mays</i>	GRMZM2G119150	64.0
<i>Z. mays</i>	GRMZM2G415117	64.7
<i>Medicago truncatula</i>	Medtr2g008430	66.9
<i>M. truncatula</i>	Medtr4g092620	67.3

^a The *ALD1*-like genes were identified by blasting (TblastN) the Arabidopsis *ALD1* protein sequence in the Phytozome v10.3 website.

^b The low level of similarity with Arabidopsis *ALD1* was due to truncated *GmALD4* enzyme caused by premature stop codon.

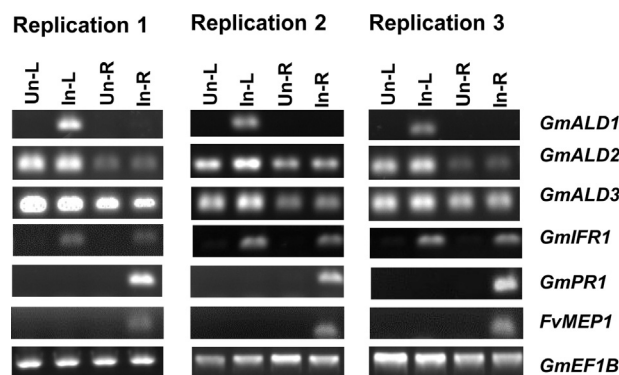


Fig. 8. Soybean *GmALD1* is transcriptionally activated in soybean leaves in response to *F. virguliforme* toxins.

RT-PCR was carried out for the following four samples. Un-L, leaves of uninfected plant; In-L, leaves of infected plants; Un-R, uninfected roots; In-R, infected roots. *GmALD1*, *GmALD2*, and *GmALD3* are three soybean homologs of Arabidopsis *ALD1* gene. Two soybean defense genes, *GmIFR1* and *GmPR1* encoding isoflavone reductase and pathogenesis-related protein, respectively, and a *F. virguliforme* gene, *FvMEP1* encoding a metalloproteinase were used as controls (Supplementary Table 1). The constitutively expressed soybean gene *GmEF1B* encoding elongation factor EF-1 beta subunit was used to determine the levels of transcripts among the samples. Results of three biological replications are presented.

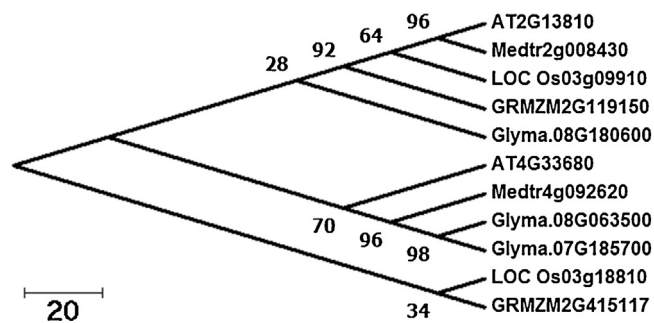


Fig. 9. Soybean *GmALD1* protein clustered with Arabidopsis *ALD1* in a clad of an un-rooted phylogenetic tree.

The tree was generated for the following Arabidopsis *ALD1*-like proteins identified from the Phytozome v10.3 website. The accession numbers of the *ALD1*-like proteins are: *Arabidopsis thaliana* AT2G13810; *A. thaliana* AT4G33680; *Glycine max* Glyma.08G180600; *G. max* Glyma.08G063500; *G. max* Glyma.07G185700; *Oryza sativa* LOC_Os03g18810; *O. sativa* LOC_Os03g09910; *Zea mays* GRMZM2G119150; *Medicago truncatula* Medtr2g008430; *M. truncatula* Medtr4g092620.

leaves of the *F. virguliforme*-infected soybean plants. We conclude that the increased Pip levels in leaves of *F. virguliforme*-infected soybean plants could be contributed from both xylem sap and local synthesis in leaf tissues. Our results also suggest that *F. virguliforme* toxins are recognized by host factors to initiate host defense mechanisms, one of which is most likely regulated by Pip.

We investigated if *ALD1* homologs of other plant species are also induced following pathogen infection. Study of the available transcriptomic data revealed that all *ALD1* homologs included in generating the phylogenetic tree are transcriptionally activated following pathogen infection (Supplementary Table 2). This observation strongly indicates that Pip may be an immunity inducer across plant species including both eudicots and monocots, and further study of this signaling molecule is warranted.

Supplementary material related to this article found, in the online version, at <http://dx.doi.org/10.1016/j.plantsci.2015.11.008>.

Conflict of interest

The authors declare to have no conflict of interests.

Acknowledgements

The authors wish to thank United Soybean Board and Ms. Katelynn Davis, Iowa State University, for technical assistance. We thank Jordan Baumbach and David Grant for reviewing the manuscript.

References

- [1] I. Abdel-Farid, M. Jahangir, C. van den Hondel, H. Kim, Y. Choi, R. Verpoorte, Fungal infection-induced metabolites in *Brassica rapa*, *Plant Sci.* 176 (2009) 608–615.
- [2] J. Kuc, Phytoalexins, stress metabolism, and disease resistance in plants, *Ann. Rev. Phytopathol.* 33 (1995) 275–297.
- [3] K. Tan, R.P. Oliver, Metabolomics and proteomics to dissect fungal phytopathogenicity, in: M. Nowrousian (Ed.), *The Mycota: Fungal Genomics*, 2nd ed., Springer, Berlin, 2014, pp. 301–319.
- [4] R.G.T. Lowe, J.W.T. Allwood, A.M. Galster, M. Urban, A. Daudi, G. Canning, J.L. Ward, M.H. Beale, K.E. Hammond-Kosack, A combined ¹H nuclear magnetic resonance and electrospray ionization mass spectrometry analysis to understand the basal metabolism of plant-pathogenic *Fusarium* spp., *Mol. Plant Microbe Interact.* 23 (2010) 1605–1618.
- [5] J. Shah, R. Chaturvedi, Z. Chowdhury, B. Venables, R. Petros, Signaling by small metabolites in systemic acquired resistance, *Plant J.* 79 (2014) 645–658.
- [6] H. Krishnan, S. Natarajan, J. Bennett, R. Sicher, Protein and metabolite composition of xylem sap from field-grown soybeans (*Glycine max*), *Planta* 233 (2011) 921–931.
- [7] N. Abeyssekara, M. Bhattacharyya, Analyses of the xylem sap proteomes identified candidate *Fusarium virguliforme* proteinaceous toxins, *PLoS One* 9 (2014) e93667.
- [8] S. Subramanian, U. Cho, C. Keyes, O. Yu, Distinct changes in soybean xylem sap proteome in response to pathogenic and symbiotic microbe interactions, *BMC Plant Biol.* 9 (2009) 119.
- [9] C. Wallis, J. Chen, Grapevine phenolic compounds in xylem sap and tissues are significantly altered during infection by *Xylella fastidiosa*, *Phytopathology* 102 (2012) 816–826.
- [10] A. Ratzinger, N. Riediger, A. von Tiedemann, P. Karlovsky, Salicylic acid and salicylic acid glucoside in xylem sap of *Brassica napus* infected with *Verticillium longisporum*, *J. Plant Res.* 122 (2009) 571–579.
- [11] J. Ward, S. Forcat, M. Beckmann, M. Bennett, S. Miller, J. Baker, et al., The metabolic transition during disease following infection of *Arabidopsis thaliana* by *Pseudomonas syringae* pv. *tomato*, *Plant J.* 63 (2010) 443–457.
- [12] J.A. Wrather, S.R. Koenning, Estimates of disease effects on soybean yields in the United States 2003 to 2005, *J. Nematol.* 38 (2006) 173–180.
- [13] T. Aoki, K. O'Donnell, Y. Homma, A. Lattanzi, Sudden-death syndrome of soybean is caused by two morphologically and phylogenetically distinct species within the *Fusarium solani* species complex: *F. virguliforme* in North America and *F. tumucumaniae* in South America, *Mycologia* 95 (2003) 660.
- [14] T. Aoki, M. Scandiani, K. O'Donnell, Phenotypic, molecular phylogenetic, and pathogenetic characterization of *Fusarium crassispitatum* sp. nov., a novel soybean sudden death syndrome pathogen from Argentina and Brazil, *Mycoscience* 53 (2012) 167–186.
- [15] K. O'Donnell, S. Sink, M. Scandiani, A. Luque, A. Colletto, M. Biasoli, et al., Soybean sudden death syndrome species diversity within North and South America revealed by multilocus genotyping, *Phytopathology* 100 (2010) 58–71.
- [16] T. Hughes, K. O'Donnell, S. Sink, A. Rooney, M. Scandiani, A. Luque, et al., Genetic architecture and evolution of the mating type locus in fusaria that cause soybean sudden death syndrome and bean root rot, *Mycologia* 106 (2014) 686–697.
- [17] K. Roy, Sudden death syndrome of soybean: *Fusarium solani* as incitant and relation of *Heterodera glycines* to disease severity, *Phytopathology* 79 (1989) 191.
- [18] J. Rupe, Frequency and pathogenicity of *Fusarium solani* recovered from soybeans with sudden death syndrome, *Plant Dis.* 73 (1989) 581.
- [19] S. Li, G. Hartman, J. Widholm, Viability staining of soybean suspension-cultured cells and a seedling stem cutting assay to evaluate phytotoxicity of *Fusarium solani* f. sp. *glycines* culture filtrates, *Plant Cell Rep.* 18 (1999) 375–380.
- [20] H. Brar, S. Swaminathan, M. Bhattacharyya, The *Fusarium virguliforme* toxin FvTox1 causes foliar sudden death syndrome-like symptoms in soybean, *Mol. Plant Microbe Interact.* 24 (2011) 1179–1188.
- [21] H. Brar, M. Bhattacharyya, Expression of a single-chain variable-fragment antibody against a *Fusarium virguliforme* toxin peptide enhances tolerance to sudden death syndrome in transgenic soybean plants, *Mol. Plant Microbe Interact.* 25 (2012) 817–824.
- [22] R. Pudake, S. Swaminathan, B. Sahu, L. Leandro, M. Bhattacharyya, Investigation of the *Fusarium virguliforme* *fvtox1* mutants revealed that the FvTox1 toxin is involved in foliar sudden death syndrome development in soybean, *Curr. Genet.* 59 (2013) 107–117.
- [23] G. Hartman, Y. Huang, R. Nelson, G. Noel, Germplasm evaluation of *Glycine max* for resistance to *Fusarium solani*, the causal organism of sudden death syndrome, *Plant Dis.* 81 (1997) 515–518.
- [24] D.A. Lightfoot, P.T. Gibson, K. Meksem, Method of determining soybean sudden death syndrome resistance in a soybean plant, US Patent 7288386 (2007).
- [25] T. Ohta, N. Masutomi, N. Tsutsui, T. Sakairi, M. Mitchell, M.V. Milburn, J.A. Ryals, K.D. Beebe, L. Guo, Untargeted metabolomic profiling as an evaluative tool of fenofibrate-induced toxicology in Fischer 344 male rats, *Toxicol. Pathol.* 37 (2009) 521–535.
- [26] M. Evans, C.D. DeHaven, T. Barrett, M. Mitchell, E. Milgram, Integrated, nontargeted ultrahigh performance liquid chromatography/electrospray ionization tandem mass spectrometry platform for the identification and relative quantification of the small-molecule complement of biological systems, *Anal. Chem.* 81 (2009) 6656–6667.
- [27] B. Welch, The generalization of 'student's' problem when several different population variances are involved, *Biometrika* 34 (1947) 28.
- [28] J. Storey, R. Tibshirani, Statistical significance for genomewide studies, *Proc. Natl. Acad. Sci. U. S. A.* 100 (2003) 9440–9445.
- [29] V. Lozovaya, A. Lygin, O. Zernova, S. Li, G. Hartman, J. Widholm, Isoflavonoid accumulation in soybean hairy roots upon treatment with *Fusarium solani*, *Plant Physiol. Biochem.* 42 (2004) 671–679.
- [30] O. Radwan, M. Li, B. Calla, S. Li, G. Hartman, S. Clough, Effect of *Fusarium virguliforme* phytotoxin on soybean gene expression suggests a role in multidimensional defence, *Mol. Plant Pathol.* 14 (2012) 293–307.
- [31] H. Weichert, I. Stenzel, E. Berndt, C. Wasternack, I. Feussner, Metabolic profiling of oxylipins upon salicylate treatment in barley leaves—preferential induction of the reductase pathway by salicylate, *FEBS Lett.* 464 (1999) 133–137.
- [32] H.W. Gardner, R. Kleiman, A soy extract catalyzes formation of 9-oxo-*trans*-12,13-epoxy-*trans*-10-octadecenoic acid from 13-hydroperoxy-*cis*-9,*trans*-11-octadecadienoic acid, *Lipids* 12 (1977) 941–944.
- [33] A. Andreou, F. Brodhun, I. Feussner, Biosynthesis of oxylipins in non-mammals, *Prog. Lipid Res.* 48 (2009) 148–170.
- [34] K.A. Aliferis, D. Faubert, S. Jabaji, A metabolic profiling strategy for the dissection of plant defense against fungal pathogens, *PLoS One* 9 (2014) e111930.
- [35] J. Ji, M. Scott, M. Bhattacharyya, Light is essential for degradation of ribulose-1,5-bisphosphate carboxylase-oxygenase large subunit during sudden death syndrome development in soybean, *Plant Biol.* 8 (2006) 597–605.
- [36] L.F. Thatcher, J.M. Manners, K. Kazan, *Fusarium oxysporum* hijacks CO11-mediated jasmonate signaling to promote disease development in *Arabidopsis*, *Plant J.* 58 (2009) 927–939.
- [37] C. Baron, P. Zambryski, The plant response in pathogenesis, symbiosis, and wounding: variations on a common theme? *Annu. Rev. Genet.* 29 (1995) 107–129.
- [38] R. Kosslak, R. Bookland, J. Barkei, H. Paaren, E. Appelbaum, induction of *Bradyrhizobium japonicum* common nod genes by isoflavones isolated from *Glycine max*, *Proc. Natl. Acad. Sci. U. S. A.* 84 (1987) 7428–7432.
- [39] M. Harrison, R. Dixon, Spatial patterns of expression of flavonoid/isoflavonoid pathway genes during interactions between roots of *Medicago truncatula* and the mycorrhizal fungus *Glomus versiforme*, *Plant J.* 6 (1994) 9–20.
- [40] M.M. Scandiani, A.G. Luque, M.V. Razori, L.C. Casalini, T. Aoki, K. O'Donnell, G.D.L. Cervigni, C.P. Spampinato, Metabolic profiles of soybean roots during early stages of *Fusarium tumucumaniae* infection, *J. Exp. Bot.* 66 (2015) 391–402.
- [41] H. Návárová, F. Bernsdorff, A. Doring, J. Zeier, Pipecolic acid, an endogenous mediator of defense amplification and priming, is a critical regulator of inducible plant immunity, *Plant Cell* 24 (2012) 5123–5141.
- [42] L. Yatsu, D. Boynton, Pipecolic acid in leaves of strawberry plant as influenced by treatments affecting growth, *Science* 130 (1959) 864–865.

- [43] G. Pálfi, L. Dézsi, Pipecolic acid as an indicator of abnormal protein metabolism in diseased plants, *Plant Soil* 29 (1968) 285–291.
- [44] M. Moulin, C. Deleu, F. Larher, A. Bouchereau, The lysine-ketoglutarate reductase saccharopine dehydrogenase is involved in the osmo-induced synthesis of pipecolic acid in rapeseed leaf tissues, *Plant Physiol. Biochem.* 44 (2006) 474–482.
- [45] D. Sandhu, I. Tasma, R. Frasch, M. Bhattacharyya, Systemic acquired resistance in soybean is regulated by two proteins, orthologous to *Arabidopsis* NPR1, *BMC Plant Biol.* 9 (2009) 105.